INFECTION AND IMMUNITY, June 2009, p. 2330–2342 Vol. 77, No. 6
0019-9567/09/$08.00+0 doi:10.1128/IAI.00057-09

Designing Therapies against Experimental Visceral Leishmaniasis by Modulating the Membrane Fluidity of Antigen-Presenting Cells▽

Subha Banerjee,[1] June Ghosh,[1] Subha Sen,[1] Rajan Guha,[1] Ranjan Dhar,[1] Moumita Ghosh,[1] Sanchita Datta,[1] Bikramjit Raychaudhury,[1] Kshudiram Naskar,[1] Arun Kumar Haldar,[1] C. S. Lal,[2] K. Pandey,[2] V. N. R. Das,[2] Pradeep Das,[2] and Syamal Roy[1]*

Indian Institute of Chemical Biology, Council of Scientific & Industrial Research, 4 Raja S.C. Mullick Road, Kolkata 700032, India,[1] and Rajendra Memorial Research Institute of Medical Sciences, Indian Council of Medical Research, Patna 800007, India[2]

Received 16 January 2009/Returned for modification 2 March 2009/Accepted 6 March 2009

The membrane fluidity of antigen-presenting cells (APCs) has a significant bearing on T-cell-stimulating ability and is dependent on the cholesterol content of the membrane. The relationship, if any, between membrane fluidity and defective cell-mediated immunity in visceral leishmaniasis has been investigated. Systemic administration of cholesterol by liposome delivery (cholesterol liposomes) in *Leishmania donovani*-infected hamsters was found to cure the infection. Splenic macrophages as a prototype of APCs in infected hamsters had decreased membrane cholesterol and an inability to drive T cells, which was corrected by cholesterol liposome treatment. The effect was cholesterol specific because liposomes made up of the analogue 4-cholesten-3-one provided almost no protection. Infection led to increases in interleukin-10 (IL-10), transforming growth factor beta, and IL-4 signals and concomitant decreases in gamma interferon (IFN-γ), tumor necrosis factor alpha, and inducible NO synthase signals, which reverted upon cholesterol liposome treatment. The antileishmanial T-cell repertoire, whose expansion appeared to be associated with protection, was presumably type Th1, as shown by enhanced IFN-γ signals and the predominance of the immunoglobulin G2 isotype. The protected group produced significantly more reactive oxygen species and NO than the infected groups, which culminated in killing of *L. donovani* parasites. Therefore, cholesterol liposome treatment may be yet another simple strategy to enhance the cell-mediated immune response to *L. donovani* infection. To our knowledge, this is the first report on the therapeutic effect of cholesterol liposomes in any form of the disease.

The disease visceral leishmaniasis or kala-azar is spreading in the Indian subcontinent and elsewhere, and evolution of antimony-resistant strains has been compounding this disaster (14). The inability of kala azar patients to mount an antileishmanial cell-mediated immune response is the hallmark of the disease (28). So far, there is no effective vaccine against kala-azar. Among the drugs used, pentamidine is toxic, amphotericin B is expensive for the target population on the subcontinent and toxic (and there have been reported cases of resistance) (67), and use of oral miltefosine is limited by cost, contraindications, and the emergence of resistance (69). In view of these limitations there is an urgent need to develop an affordable therapy. The work presented here is directed toward this goal. The idea that cholesterol-rich liposomes may have a therapeutic role in treatment of leishmaniasis stems from our previous finding that during their intracellular life cycle *Leishmania* parasites disrupt the membrane rafts of macrophages (MΦs) by increasing membrane fluidity. The increase in fluidity, when corrected physically by exposing the parasitized MΦs to a temperature lower than the phase transition temperature or chemically by liposomal delivery of cholesterol, leads to correction of antigen presentation (10). This encouraging result, coupled with the fact that cholesterol has been identified as a potential therapeutic agent for use against leishmania infection (50), brought into focus the therapeutic efficacy of cholesterol-rich liposomes in *Leishmania donovani*-infected hamsters. Cholesterol therapy is in clinical use either directly or as an adjunct to treatment. Compared to drug treatment alone, a cholesterol-rich diet together with an antitubercular drug increased the rate of sterilization of sputum in patients having pulmonary tuberculosis (48). Patients with Smith-Lemli-Opitz syndrome who were treated with a pure cholesterol suspension orally showed improvement in symptoms associated with the disease (16).

The role of membrane cholesterol in the T-cell—antigen-presenting cell (APC) interaction has been well studied in various systems. Cholesterol depletion results in inhibition of phytohemagglutinin-dependent lymphocyte cytotoxicity against allogeneic target cells, and the opposite effect is observed after cholesterol enrichment (15). Cholesterol treatment enhances the antigen-presenting function of monocytes by upregulating the expression of major histocompatibility complex (MHC) class II (25), promotes phagocytosis of *Helicobacter pylori* by APCs, and enhances an antigen-specific T-cell response during bacterial challenge, leading to a T-cell-dependent reduction in the number of bacteria in the stomach (68). Treatment of APCs with nystatin or methyl cyclodextrin, which are known quenchers of cholesterol from the membrane, reduces the antigen-presenting ability without affecting the cell surface expression of class II molecules (4). Thus, cholesterol may play a decisive role in the cell-mediated immune response of the host. Membrane cholesterol regulates membrane-

* Corresponding author. Mailing address: Indian Institute of Chemical Biology, Council of Scientific & Industrial Research, Kolkata 700032, India. Phone: 091-033-2473-3491. Fax: 091-033-2473-0284. E-mail: sroy@iicb.res.in.

▽ Published ahead of print on 16 March 2009.

embedded receptors in terms of their affinity state, binding capacity, and signal transduction (9). Cholesterol is necessary for raft assembly (59), which is intimately involved in the dynamics of immune synapse formation, an essential event in T-cell receptor-mediated signal transduction (52). Recently, it was shown that the level of serum cholesterol decreased during the active stage of kala azar but that the levels of all the lipid parameters returned to the normal reference ranges after successful chemotherapy (33).

As a part of our continuing search for new horizons for kala azar therapy, we studied the therapeutic role, if any, of liposomal delivery of cholesterol in *L. donovani*-infected hamsters (I-hamsters). This was expected to allow us to examine a number of cholesterol-induced cellular phenomena associated with the antileishmanial immune response and protection.

MATERIALS AND METHODS

Antibodies and other reagents. Biotin-conjugated mouse anti-Armenian and anti-Syrian hamster immunoglobulin G1 (IgG1) monoclonal antibody (MAb) and avidin-horseradish peroxidase-conjugated mouse anti-Syrian hamster IgG2 MAb were obtained from BD Biosciences. Penicillin, streptomycin, sodium bicarbonate, HEPES, 2-mercaptoethanol, fura-2-acetoxymethyl ester, paraformaldehyde, fluorescein isothiocyanate (FITC)-conjugated cholera toxin B subunit (CTXB-FITC), 2,2′-azinobis(3-ethylbenzthiazoline-6-sulfonate) (ABTS), a PKH26 cell-labeling kit, sulfanilamide, *N*-(1-naphthyl)ethylene diamine hydrochloride, Giemsa stain, Bradford's reagent, EDTA, and RPMI 1640 were purchased from Sigma Aldrich (St. Louis, MO). Phosphatidylcholine (PC) (egg lecithin) and 4-cholesten-3-one were purchased from ICN (Irvine, CA). Anti-kinetoplastid membrane protein 11 (KMP-11) MAb (mouse IgG1) was obtained from Cedarlane Lab (Ontario, Canada). FITC-conjugated anti-mouse IgG was obtained from Jackson Laboratories, United States. Cholesterol, hydrogen peroxide, and Tween 20 were obtained from Merck. [^{3}H]thymidine (specific activity, 6.7 Ci/mmol) was purchased from New England Nuclear, Boston, MA. 2′,7′-Dichlorodihydrofluorescein diacetate was obtained from Molecular Probes (Eugene, OR). Preservative-free sodium antimony gluconate (SAG) was a kind gift from Albert David Ltd. (Kolkata, India).

Propagation of parasite, infection of hamsters, determination of the parasite burden, and preparation of SLA. Golden hamsters (4 to 6 weeks old) were obtained from the animal facility of the Indian Institute of Chemical Biology. They were housed under conventional conditions with food and water provided ad libitum, and they were used for experiments with prior approval of the institutional animal ethics committee. *L. donovani* strain AG83 (MAOM/IN/1083/AG83), originally obtained from an Indian kala-azar patient, was used to infect 4- to 6-week-old hamsters with either amastigotes or promastigotes (5×10^6 parasites/animal) by the intracardiac route (44). Splenic and hepatic parasite burdens in hamsters were determined by the stamp smear method as described previously (61); the results are expressed as numbers of parasites per spleen and numbers of parasites per liver, respectively. Soluble leishmanial antigen (SLA) was prepared after sonication of promastigotes as described previously (57).

Liposome preparation, visualization by TEM, measurement of size, systemic delivery of liposomes, and injection of sub-SAG. Liposomes were prepared from PC and either cholesterol or an analogue of cholesterol (4-cholesten-3-one) at a molar ratio of 1:1.5 (60). Briefly, 5.8 mg cholesterol or 4-cholesten-3-one and 8 mg PC were dissolved in chloroform, and a thin film was prepared; subsequently, the film was dissolved in 1 ml saline and sonicated (Microson Ultrasonic cell disruptor with a Misonix 2-mm probe) at 4°C three times for 1 min each time at maximum output (10). A mixture of cholesterol and PC was also prepared without sonication and designated an emulsion. To obtain a visual impression, the morphologies of liposomes and emulsions were studied by performing transmission electron microscopy (TEM) (FEI, The Netherlands) after negative staining of samples with uranyl acetate (32). The size distributions of liposomes were determined by measuring the diameters of about 300 liposomes at random using TEM. To obtain information about lamellation, liposomes in phosphate-buffered saline (PBS) were mixed with an equal volume of 3% agar and kept at −20°C overnight. The solidified agar containing vesicles was cut into sections that were 60 nm thick with a cryoultramicrotome (Leica) (23). Sections were stained with uranyl acetate and then examined by TEM. A liposome prepared from cholesterol and PC was designated a cholesterol liposome. Similarly, a liposome prepared from 4-cholesten-3-one and PC was designated an analogue liposome. Liposomes (200 μl of a liposomal suspension or emulsion) were injected into I-hamsters via the intracardiac route as described previously (40). A suboptimal dose of SAG (sub-SAG) was injected into I-hamsters on days 7, 14, and 21 (day 0 was defined as the date of infection) at a dose of 50 mg/kg (body weight) (21).

Preparation of splenic adherent cells and analysis of their purity. Splenic adherent cells from hamsters were purified by using an adherence procedure as described previously (56). To analyze the purity, the phagocytic ability of sheep red blood cells (SRBC) was studied (56). When preparations were observed under a microscope, 95% of the adherent cells were phagocytic, as shown by the presence of intracellular SRBC. As antibodies (Abs) for characterization of hamster cells are not available, it was not possible to characterize these adherent cells any further. For convenience, these adherent cells are referred to below as splenic MΦs.

Quantification of membrane cholesterol with an Amplex Red assay kit. The MΦ membrane was prepared as described previously (27), with some modifications. Briefly, homogenization of MΦs was carried out by repeated freezing and thawing, and the postnuclear supernatant was harvested by centrifugation at $100{,}000 \times g$. The resulting precipitate was considered the membrane fraction. The protein content of the membrane was determined as described previously (37). The cholesterol content was determined by using an Amplex Red reagent kit (2), and the results were expressed in μM cholesterol/μg protein.

T-cell proliferation assay. Single-cell suspensions of splenocytes from different experimental groups of hamsters were prepared after Ficoll density gradient centrifugation and then suspended in complete RPMI 1640. Cells were plated in triplicate at a concentration of 10^5 cells/well in 96-well plates and allowed to proliferate for 3 days at 37°C in a 5% CO_2 incubator either in the presence or in the absence of SLA (5 μg/ml) (6). For concanavalin A (ConA)-induced proliferation, the mitogen was added at a concentration of 5 μg/ml as described previously (6). At 18 h before harvest, cells were pulsed with 1 μCi [^{3}H]thymidine/well, whose uptake (as an index of proliferation) was measured with a liquid scintillation counter (Tri-Carb 2100TR; Packard Instruments) as described previously (6).

Analysis of expression of endogenous leishmanial antigen. Expression of KMP-11 as an endogenous leishmanial antigen in MΦs was checked by staining with anti-KMP-11 MAb. MΦs from normal hamsters, I-hamsters, and cholesterol liposome-treated I-hamsters (L-I-hamsters) were stained with anti-KMP-11 mouse MAb and then with FITC-conjugated anti-mouse IgG. Stained cells were then observed with a fluorescence microscope (Leica DMLB).

Generation of anti-KMP-11 T-cell line (T^{KMP}). A KMP-11-expressing mammalian expression vector construct (PCMV-LIC KMP-11) was used for immunization (6). A T-cell line was developed by repeated stimulation of primed T cells with SLA (54). Hamsters were primed with KMP-11 DNA intramuscularly (with two 150-μg booster doses of the plasmid 7 days apart). Spleen cells were collected 1 month after priming and were stimulated with SLA (5 μg/ml) for 2 weeks. The viable cells were purified by using Ficoll-Hypaque, restimulated with irradiated (3,000 rads; BI 2000 BRIT, Mumbai, India) spleen cells (5×10^6 cells/ml), and kept for another 2 weeks in the presence of SLA (5 μg/ml). The cycle was repeated once more to enrich antigen-specific T cells. Blasted cells purified by using Ficoll-Hypaque were designated anti-KMP-11 T-cell line T^{KMP} and used for subsequent studies.

Analysis of conjugate formation by confocal microscopy. To study conjugate formation, MΦs and T^{KMP} cells were labeled with CTXB-FITC and PKH26, respectively, as described previously (10). The stained MΦs and T^{KMP} cells were mixed at a ratio of 1:5, resuspended in PBS containing 5% fetal calf serum, and allowed to form conjugates for 30 min. The cells were then fixed with 1% paraformaldehyde, mounted with 90% glycerol on a glass slide, and observed with a confocal microscope (LSM 510; Zeiss). Cells found to be joined in couplets by phase-contrast microscopy and exhibiting a zone of colocalization as determined by confocal microscopy were considered to have formed a synapse. The number of synapse-forming couplets per 100 MΦs was expressed as the percentage of synapse formation.

Intracellular Ca^{2+} mobilization in T cells and assay of IL-2. To determine if the synapses formed were true synapses, intracellular Ca^{2+} mobilization in T^{KMP} cells and the resulting interleukin-2 (IL-2) production were monitored using MΦs derived either from I-hamsters (I-MΦs) or from L-I-hamsters (L-I-MΦs) as APCs without any exogenous antigen (KMP-11). Briefly, T-cells were resuspended in PBS containing 6 μM fura-2-acetoxymethyl ester for 60 min at 37°C in the dark with gentle shaking. The cells were washed with Hanks balanced salt solution and resuspended in Hanks balanced salt solution containing 0.5 μM EGTA at a concentration of 10^6 cells/ml. The cell suspension (1 ml) was placed in a continuously stirred cuvette at room temperature in a fluorimeter (Hitachi U440). After ~1 min of scanning, appropriate APCs were added to the cuvette, and fluorescence was monitored in real time using excitation wavelengths of 340 nm and 380 nm and an emission wavelength of 510 nm with a bandwidth of 10 nm. The data were expressed as the relative ratio of fluorescence excitation at

340 to fluorescence excitation at 380 nm (55). Similarly, T^{KMP} cells were mixed with APCs as described above and incubated at 37°C for 24 h, and the resulting IL-2 present in the culture supernatant was assayed by determining the [^{3}H] thymidine uptake using the HT-2 cell line as previously described (10).

Measurement of antileishmanial Ab responses. Serum samples were obtained from different groups of hamsters (six animals per group) and analyzed to determine the SLA-specific Ab titer. Ninety-six-well enzyme-linked immunosorbent assay (ELISA) plates (Nunc) were coated with SLA (2 μg/ml) in PBS overnight at 4°C. The plates were blocked with 5% fetal calf serum in PBS at room temperature for 1 h to prevent nonspecific binding. Sera from different groups of hamsters were added at various dilutions and incubated for 2 h at room temperature. Sera were diluted 10^{-1}, 10^{-2}, and 10^{-3} for determination of IgG1 and 10^{-3}, 10^{-4}, and 10^{-5} for determination of IgG2. Biotin-conjugated mouse anti-hamster IgG1 and mouse anti-Armenian and anti-Syrian hamster IgG2 were added and incubated for 1 h at room temperature; this was followed by 1 h of incubation with the detection reagent (avidin-conjugated horseradish peroxidase). As a peroxide substrate in citrate buffer (0.1 M, pH 4.3), ABTS was added along with 0.1% H_2O_2 to a 96-well plate, and the absorbance at 405 nm was read with an ELISA plate reader (DTX 800 multimode detector: Beckman Coulter) (6).

RNA isolation and semiquantitative reverse transcription (RT)-PCR analysis of cytokines and iNOS. Splenocytes were isolated using the RNeasy minikit procedure (Qiagen) as described previously (6). The forward and reverse primers were used to amplify cytokine transcripts. All of these hamster-specific primers except the inducible NO synthase (iNOS) primer were originally described by Melby et al. (42). The following forward and reverse primers were used: for IL-10, forward primer 5′ACAATAACTGCACCCACTTC3′ and reverse primer 5′AGGCTTCTATGCAGTTGATG3′ (432-bp product); for IL-4, forward primer 5′CATTGCATYGTTAGCRTCTC3′ and reverse primer 5′TTCCAGG AAGTCTTTCAGTG3′ (463-bp product); for gamma interferon (IFN-γ), forward primer 5′GGATATCTGGAGGAACTGGC3′ and reverse primer 5′CGA CTCCTTTTCCGCTTCCT3′ (309-bp product); for tumor necrosis factor alpha (TNF-α), forward primer 5′GACCACAGAAAGCATGATCC3′ and reverse primer 5′TGACTCCAAAGTAGACCTGC3′ (695-bp product); and for transforming growth factor beta (TGF-β), forward primer 5′CCCTGGAYACCAAC TATTGC3′ and reverse primer 5′ATGTTGGACARCTGCTCCAC3′ (310-bp product). To obtain specific amplification for iNOS, the following specific primers were used (6): forward primer 5′ GCAGAATGTGACCATCATGG3′ and reverse primer 5′CTCGAYCTGGTAGTAGTAGAA3′ (198-bp product). For hypoxanthine-guanine phosphoribosyl transferase (HGPRT) amplification the following primers were used (42): forward primer 5′ATCACATTATGGCCCT CTGTG3′ and reverse primer 5′CTGATAAAATCTACAGTYATGG3′ (125-bp product). Degenerate bases are indicated above by International Union of Pure and Applied Chemistry designations (Y = C or T; R = A or G). Samples (1 μg) of RNA from different experimental groups of hamsters were first utilized for cDNA synthesis with reverse primers (IDT; Sigma) using mouse Moloney leukemia virus reverse transcriptase (Invitrogen) at 37°C for 90 min. A common master mixture containing deoxynucleoside triphosphates (Promega) and *Taq* polymerase (Invitrogen), as well as gene-specific primers and 0.25 volume of cDNA, was used for amplification with an Applied Biosystems thermocycler. The cycling conditions for genes of interest were 5 min at 95°C, followed by 40 cycles of denaturation at 95°C for 30 s, annealing at 56°C for 40 s, and extension at 72°C for 40 s. The identities of the PCR-amplified gene products were verified by agarose gel electrophoresis. Identical aliquots were processed in parallel without reverse transcriptase to rule out the presence of residual genomic DNA contamination in PCR amplification preparations. Densitometric analyses were done using the Quantity One software (Bio-Rad), ethidium bromide staining, and visualization under a UV transilluminator. For densitometric calculations, the same band area was used to determine band intensity and normalized for HGPRT.

Measurement of ROS and NO. To monitor the level of reactive oxygen species (ROS) (including superoxide, hydrogen peroxide, and other reactive oxygen intermediates), the cell-permeable, nonpolar, H_2O_2-sensitive probe 2′,7′-dichlorofluorescin diacetate was used (43). The extent of H_2O_2 generation was defined as the extent of ROS generation for convenience. For each experimental sample, fluorometric measurements were performed in triplicate, and the results were expressed asin the mean fluorescence intensity per 10^6 cells. Nitric oxide (NO) generation was monitored by using the Griess reaction as described previously (22), and the results were expressed in μM nitrite.

Treatment strategy. Previously, we have shown that in I-hamsters there is essentially a linear increase in the parasite load in the spleen and liver from 45 days to 120 days postinfection (44). Hamsters infected for 45 days (with promastigotes) and for 60 days (with lesion-derived amastigotes) were used in our study. The hamsters infected for 45 days were divided into six groups (groups I to VI). Group I received only saline, whereas groups II to VI received cholesterol liposomes, analogue liposomes, the emulsion, sub-SAG, and cholesterol liposomes together with sub-SAG (L-I-sub-SAG-hamsters), respectively. All the animals were sacrificed 30 days after they received the treatment, when splenic and hepatic parasite burdens were determined.

Survival kinetics. To evaluate long-term therapeutic applicability, 25 I-hamsters, 20 L-I-hamsters, and 20 L-I-sub-SAG-hamsters were used to study survival kinetics as described previously (44).

Statistical analysis. The statistical significance of differences between groups was determined by the unpaired two-tailed Student *t* test. Statistical significance was defined as a P value of <0.05, and results were expressed as averages and standard deviations of triplicate measurements.

RESULTS

Characterization of liposomes. Liposomes were prepared from PC either with cholesterol (Fig. 1A) or with its analogue 4-cholesten-3-one (Fig. 1E) and were designated cholesterol liposomes (Fig. 1B) and analogue liposomes (Fig. 1F), respectively. TEM confirmed that liposomes were indeed formed upon sonication. The size distributions of liposomes were studied immediately after preparation. The vesicles were almost spherical, and the majority of them fell in the size ranges from 60 to 110 nm and from 40 to 115 nm for cholesterol liposomes (Fig. 1G) and analogue liposomes (Fig. 1H), respectively (modal sizes, 70 nm and 80 nm, respectively). Ultrathin sections of liposomes were prepared and viewed by TEM, which revealed that the cholesterol liposomes were unilamellar vesicles (Fig. 1C). Seemingly, there was no liposome formation in the cholesterol-PC preparation which was not subjected to sonication, and the resulting suspension was defined as an emulsion which had a dispersed distribution of lipid without any defined structure (Fig. 1D).

Delivery of cholesterol liposomes but not analogue liposomes reduced the organ parasite burden in hamsters infected with promastigotes. There was a significant decrease in the hepatic parasite burden in response to cholesterol liposome treatment (group II) compared to I-hamsters (group I) ($P < 0.001$ for experiments i to iii), whereas analogue liposome treatment (group III) protected animals on only one occasion (experiment i; $P < 0.05$) and emulsion treatment (group IV) provided no protection (Fig. 2). On the other hand, sub-SAG treatment of I-hamsters (group V) provided protection on two occasions ($P < 0.01$ and < 0.001 for experiments i and iii, respectively). In the case of L-I-sub-SAG-hamsters (group VI) there was slight enhancement of the efficacy compared to cholesterol liposome-treated hamsters, but the level of significance was the same. Cholesterol liposome treatment also resulted in a significant decrease in the parasite load in the spleen ($P < 0.01$ for experiments i and iii and $P < 0.05$ for experiment ii). Neither cholesterol analogue nor emulsion treatment of I-hamsters offered any protection (Fig. 2). However, the data for sub-SAG treatment showed wide variation in the results ($P < 0.01$ for experiments i and iii) (Fig. 2). Clearance of splenic parasites upon L-I-sub-SAG treatment showed some variation ($P < 0.01$, $P < 0.05$, and $P < 0.001$ for experiments i, ii, and iii, respectively) compared to the results for the hepatic parasite burden ($P < 0.001$, $P < 0.001$, and $P < 0.001$ for experiments i, ii, and iii, respectively).

Delivery of cholesterol liposomes but not delivery of analogue liposomes reduced the organ parasite burden in hamsters infected with amastigotes. Promastigotes are known to be

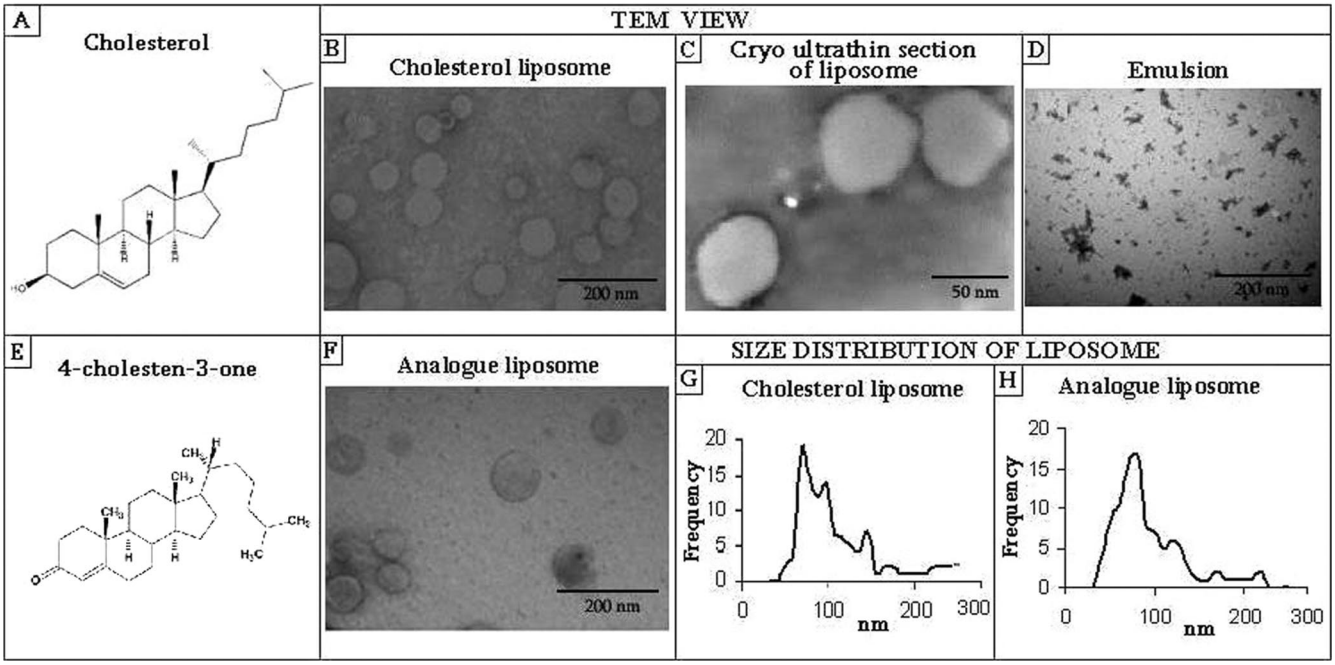

FIG. 1. TEM micrographs of liposomes and lipid emulsions and their size distributions. (A and E) Chemical structures of cholesterol (A) and 4-cholest-3-one (E). A mixture of cholesterol and PC at a molar ratio of 1.5:1 was either sonicated to prepare liposomes (cholesterol liposomes) (B) or not sonicated (emulsion) (D). (C) Section of liposomes showing lamellation. (F) Similarly, 4-cholesten-3-one, the cholesterol analogue, was mixed with PC at a molar ratio of 1.5:1 and sonicated to prepare analogue liposomes. (F and G) The size distributions of cholesterol liposomes (G) and analogue liposomes (H) were analyzed by using TEM and were determined at random by measuring the diameters of 300 individual liposomes. Magnification, ×43,500.

at least 1 log less infective than amastigotes (29). Thus, we studied the effects of cholesterol liposome, analogue liposome, sub-SAG, and L-I-sub-SAG treatments in hamsters infected with amastigotes. As expected, the organ parasite load was significantly greater when animals were infected with amastigotes than when animals were infected with promastigotes. Hamsters infected for 60 days were divided into five groups and were treated with saline (group I), cholesterol liposomes (group II), analogue liposomes (group III), sub-SAG (group IV), and L-I-sub-SAG (group V). Two independent experiments were performed (experiments i and ii). Cholesterol liposome treatment of I-hamsters resulted in a significant reduction in the parasite burden both in the liver ($P < 0.05$ and $P < 0.001$ for experiments i and ii, respectively) and in the spleen ($P < 0.01$ and $P < 0.001$ for experiments i and ii, respectively), although the effect was more pronounced in the spleen. As anticipated, analogue liposome treatment provided almost no protection. Sub-SAG treatment caused a significant reduction in the parasite burden in the liver ($P < 0.05$ and $P < 0.01$ for experiments i and ii, respectively) and in the spleen ($P < 0.05$ and $P < 0.01$ for experiments i and ii, respectively). Interestingly, L-I-sub-SAG treatment tended to lower the parasite burden further compared to cholesterol liposome treatment alone, but the level of significance remained the same (Fig. 3).

Cholesterol liposome treatment reversed antileishmanial T-cell anergy. Patients with kala azar develop immune suppression (47), and the same is true for experimental infection of hamsters (16). As a measure of the cell-mediated immune response, proliferation of splenocytes with leishmanial antigens (SLA) was studied in the hamster model. The results of this study reinforced similar observations made with splenocytes of I-hamsters which failed to respond to SLA. It was observed that splenocytes of a cholesterol liposome-treated group showed a significant antileishmanial T-cell response to SLA ($P < 0.05$), suggesting that there was an expansion of the antigen-specific T-cell repertoire due to cholesterol liposome treatment (Fig. 4), but the splenocytes of analogue liposome- or lipid emulsion-treated groups failed to respond. Furthermore, splenocytes of hamsters receiving sub-SAG also responded to SLA ($P < 0.05$), whereas splenocytes of hamsters receiving cholesterol liposomes and sub-SAG showed vigorous antileishmanial proliferation ($P < 0.001$). These observations indicated that for expansion of the T-cell repertoire, cholesterol needs to be delivered in the form of liposomes and not as an emulsion. Furthermore, L-I-sub-SAG treatment had additive effects on the expansion of the antileishmanial T-cell repertoire (Fig. 4). To determine if there is generalized immune suppression in I-hamsters, we tested the ability of splenocytes to respond to ConA. It was observed that the splenocytes of I-hamsters failed to display a proliferative response to ConA, but this behavior was reversed upon cholesterol liposome treatment ($P < 0.01$). There was low but significant proliferation of splenocytes in groups treated with analogue liposomes ($P < 0.01$), the emulsion ($P < 0.001$), and sub-SAG ($P < 0.01$). Interestingly, L-I-sub-SAG-hamsters showed significantly enhanced proliferation ($P < 0.001$) of splenocytes with ConA (Fig. 4B), suggesting that the immune suppression seen in experimental visceral leishmaniasis is generalized and can be reversed by cholesterol liposome treatment. Analogue lipo-

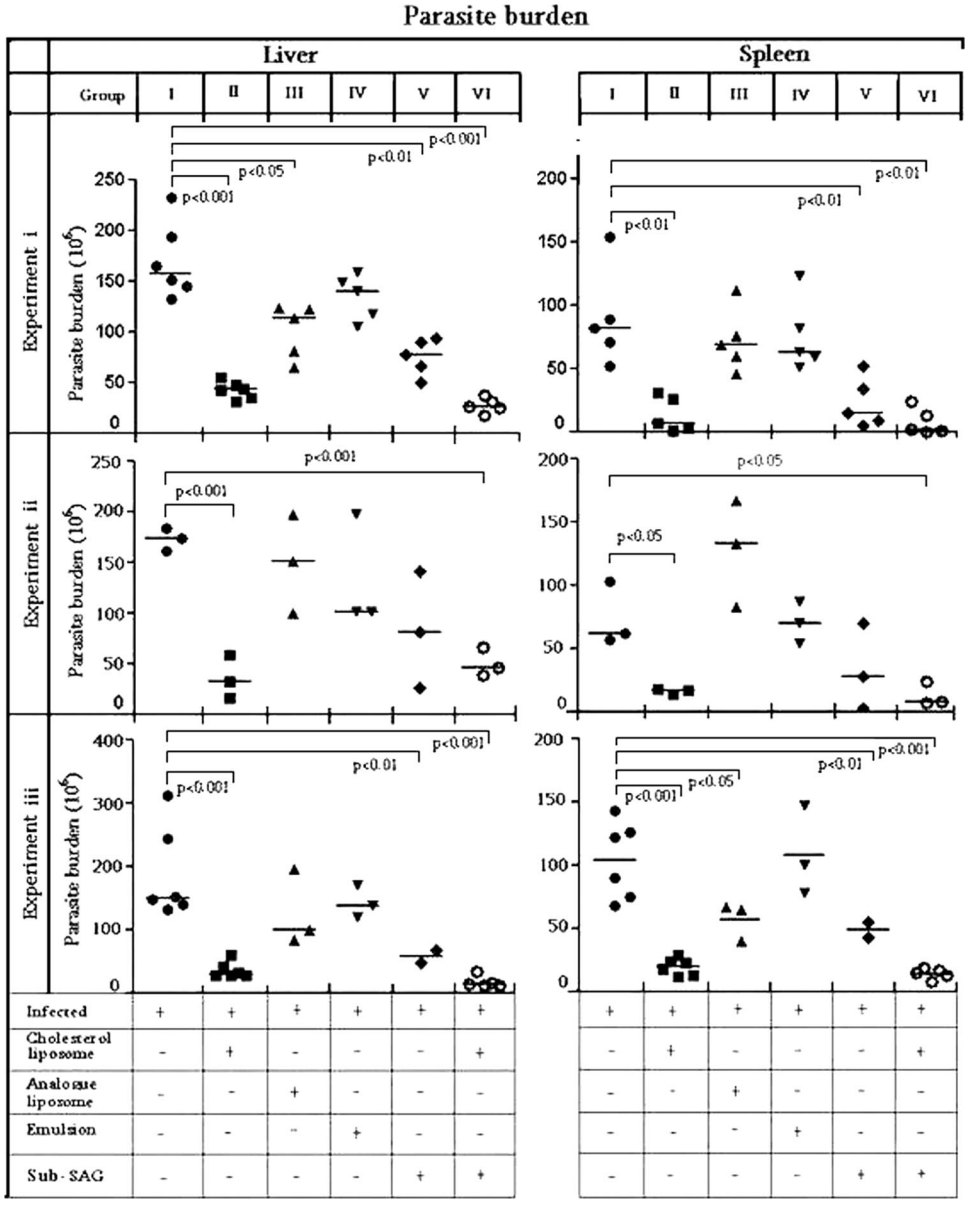

FIG. 2. Parasite burdens in the spleen and liver of hamsters infected with promastigotes. The groups and their treatments are indicated at the top and bottom, respectively. Hamsters infected for 45 days (group I) received the following treatments: cholesterol liposomes (group II), analogue liposomes (group III), emulsion (group IV), sub-SAG (group V), and a combination of cholesterol liposomes and sub-SAG (group VI). SAG was administered intramuscularly at a dose of 50 mg/kg (body weight) on days 7, 14, and 21. All the hamsters were sacrificed 30 days after liposome treatment, and the parasite burdens in the spleen and liver were determined. Each data point indicates the parasite burden in a hamster either in the spleen or in the liver. The results of three representative experiments (experiments i, ii, and iii) are shown.

some and emulsion treatments reversed the generalized immune suppression but had no effect on the antigen-specific suppression. This observation indicated that cholesterol liposome treatment but not analogue liposome treatment can drive both antigen-specific and nonspecific T cells.

The level of membrane cholesterol decreased due to infection and was restored by cholesterol liposome treatment. The status of cholesterol in the MΦ membrane was assessed by direct chemical measurement using an Amplex Red assay kit (2). There was a significant decrease in the level of membrane cholesterol due to infection ($P < 0.05$), and the level was restored by cholesterol liposome treatment but not by analogue liposome treatment (Fig. 5).

Expression of endogenous leishmanial antigen, formation of an APC—T-cell conjugate, mobilization of intracellular Ca^{2+}, and production of IL-2. We have shown that *L. donovani*-infected human monocytes can act as anti-KMP-11 peptide-specific cytotoxic T-lymphocyte targets without exogenous KMP-11 (7). The expression of KMP-11 on splenic I-MΦs and L-I-MΦs was therefore studied. The MΦs were stained with anti-KMP-11 Ab, and the binding was monitored by using FITC-conjugated anti-mouse IgG. The results demonstrate

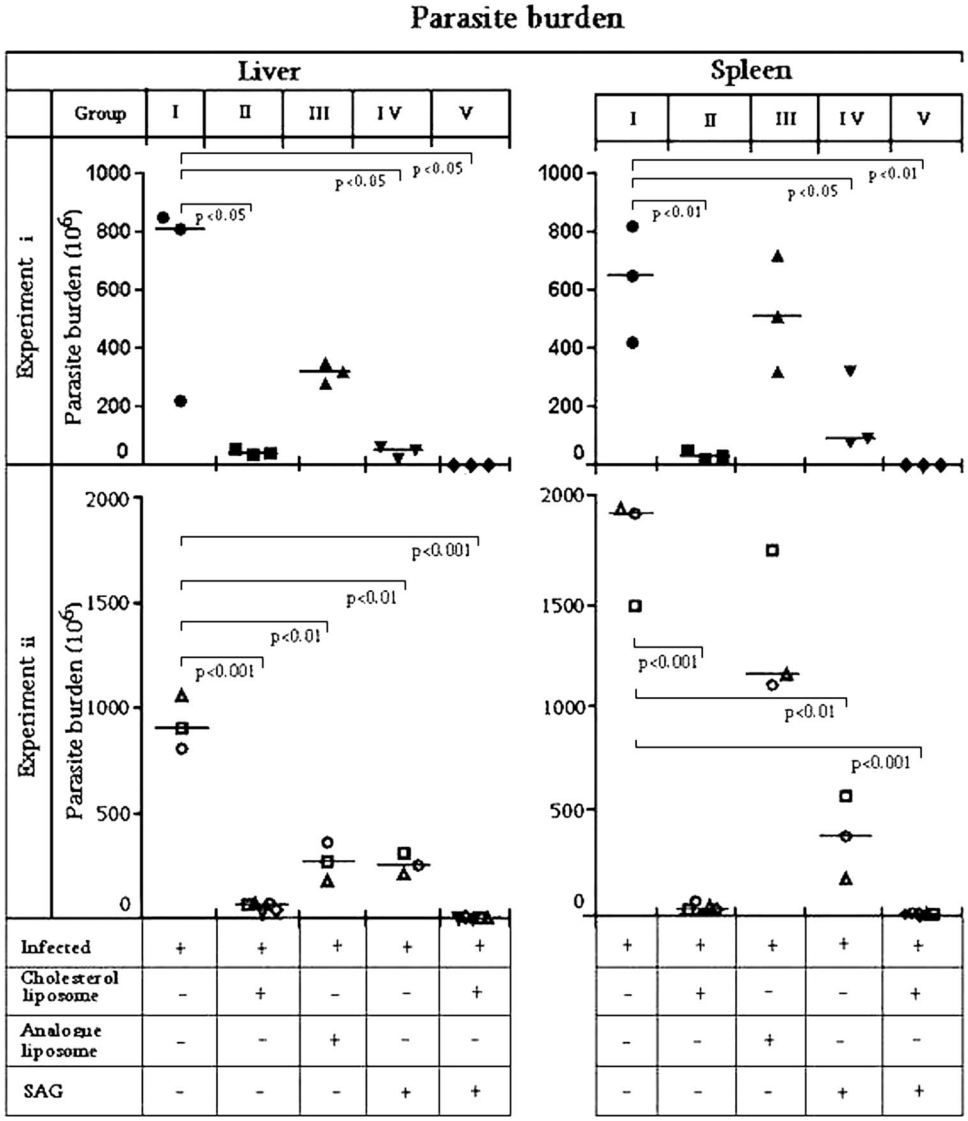

FIG. 3. Parasite burdens in the spleen and liver of hamsters infected with amastigotes. The groups and their treatments are indicated at the top and bottom, respectively. Hamsters infected for 60 days (group I) received the following treatments: cholesterol liposomes (group II), analogue liposomes (group III), sub-SAG (group IV), and a combination of cholesterol liposomes and sub-SAG (group V). SAG was administered as described in the legend to Fig. 2. All the hamsters were sacrificed 30 days after liposome treatment, and the parasite burdens in the spleen and liver were determined. The results of two representative experiments (experiments i and ii) are shown.

that both I-MΦs and L-I-MΦs show expression of KMP-11 (Fig. 6). It was also observed that the signal for KMP-11 staining was somewhat weaker in I-MΦs than in L-I-MΦs. The ability of I-MΦs and L-I-MΦs to form synapses with T^{KMP} cells was also investigated. Optimal synapse formation was observed at ~30 min. The levels of conjugate formation with I-MΦs and L-I-MΦs were 2% and 20%, respectively (Fig. 6). To show that the synapse formed was a true synapse, intracellular Ca^{2+} mobilization in T cells and IL-2 production in T^{KMP} cells were studied under identical conditions. Increases in both intracellular Ca^{2+} mobilization in T cells and IL-2 production in the supernatant were observed when T^{KMP} cells were stimulated with L-I-MΦs but not when T^{KMP} cells were stimulated with I-MΦs (Fig. 6). This very clearly indicated that L-I-MΦs, but not I-MΦs, can serve as APCs to drive T cells.

Cholesterol liposome treatment increased IFN-γ, iNOS, and TNF-α levels but decreased IL-4, IL-10, and TGF-β levels in splenocytes. The ability of cytokines and iNOS to undergo modulation in L-I-hamsters was compared to the ability of cytokines and iNOS to undergo modulation in I-hamsters by profiling cytokine gene expression. Representative data for six independent hamsters in each group are shown in Fig. 7A and B. The results generated from a densitometry analysis of each hamster were collectively expressed as means ± standard deviations for each cytokine, and the statistical significance between groups was determined (Fig. 7C). Comparative cytokine analysis showed that the expression of IFN-γ transcripts, the expression of TNF-α transcripts, and the expression of iNOS transcripts were 2.5, 2.74, and 2.26 times higher, respectively, in L-I-hamsters than in I-hamsters, whereas the levels of IL-4,

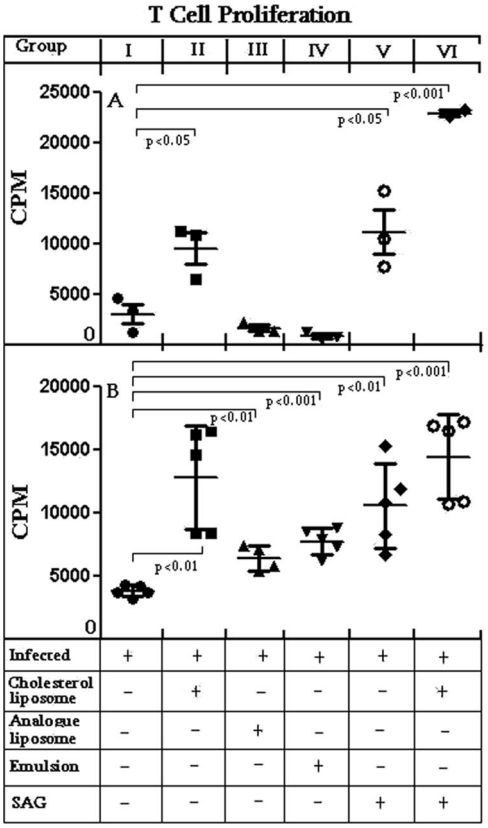

FIG. 4. Lymphoproliferation of splenocytes in response to SLA at a concentration of 5 μg/ml (A) and to the nonspecific mitogen ConA (B). The proliferative response was analyzed by using [^{3}H]thymidine incorporation. The background counts for medium alone varied between 500 and 1,000 cpm. Two experiments were conducted separately, and the data show the results of one representative experiment. The groups indicated at the top are the groups described in the legend to Fig. 2.

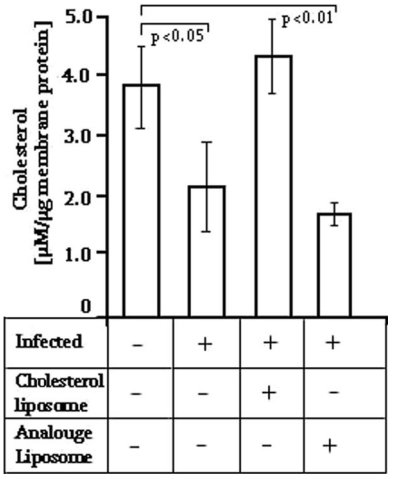

FIG. 5. Quantification of MΦ membrane cholesterol. MΦs (about 90% of the cells were phagocytic with SRBC) from five or six hamsters were pooled. The status of cholesterol in the MΦ membrane was assessed by direct chemical measurement using an Amplex Red assay kit. The bars indicate averages of triplicate measurements, and the error bars indicate standard deviations.

TGF-β, and IL-10 transcripts were 2.5-, 13-, and 2-fold lower, respectively (Fig. 7C). Studies of the ratio of IFN-γ to TGF-β and the ratio of IFN-γ to IL-10 revealed that the IFN-γ/TGF-β ratio was 35-fold greater in L-I-hamsters than in I-hamsters (Fig. 7D). Similarly, the IFN-γ/IL-10 ratio was 3.65-fold greater in L-I-hamsters than in I-hamsters (Fig. 7D).

Cholesterol liposome treatment induced generation of ROS and NO. Generation of nitrite and generation of superoxides are the main intracellular killing mechanisms for leishmanial parasites in the MΦs (1). A recent ex vivo study showed that SLA is more efficient in stimulating production of NO (58). Previously, we found that maximum ROS and NO production occurred with 5 μg/ml of SLA (6). Therefore, splenocytes were stimulated with SLA, and the resulting ROS production and NO production were recorded. There was a small but significant increase in NO production from the splenocytes of L-I-hamsters compared to the splenocytes of I-hamsters ($P < 0.05$), which was accentuated when cholesterol liposome treatment was combined with sub-SAG treatment ($P < 0.001$); this finding correlated well with the observed protection (Fig. 8). ROS production in splenocytes was significantly increased ($P < 0.001$) in L-I-hamsters and was not enhanced when this treatment was combined with sub-SAG treatment ($P < 0.01$). However, sub-SAG treatment alone resulted in great variation in ROS generation. Interestingly, treatment with analogue liposomes or the emulsion also induced a low level of ROS generation ($P < 0.05$) (Fig. 8). When L-I-hamster, analogue liposome-treated, and emulsion-treated groups were compared, there was no significant difference in NO production, whereas there was considerably greater ROS generation in L-I-hamsters than in hamsters in the other two groups ($P < 0.01$) (Fig. 8).

Cholesterol delivery increased the antileishmanial IgG2/IgG1 ratio. As no information is available for the helper T-cell subsets in hamsters, we studied the Ig isotypes in sera of hamsters to indirectly assess how T-cell subsets undergo changes during the active stage of the disease and during protection. Although there are no distinct classifications of Ig in hamsters, it is believed that hamster IgG2 corresponds to mouse IgG2a/IgG2b and hamster IgG1 corresponds to murine IgG1 (16). There was an increase in the IgG2 level in protected hamsters compared to the infected group, but there was not much variation in the IgG1 level in normal, infected, and protected hamsters. Because the IgG2 titer was much higher than the IgG1 titer, the sera used for IgG2 determination were diluted 10^{-3}-, 10^{-4}-, and 10^{-5}-fold, whereas the sera used for IgG1 determination were diluted 10^{-1}-, 10^{-2}-, and 10^{-3}-fold (Fig. 9). Even with progressive dilution, the IgG1 titer remained essentially the same. We therefore determined the median ratio of IgG2 to IgG1 for the 10^{-3} dilution of serum; the median was determined for only the 10^{-3} dilution of serum for all the groups. The ratios of IgG2 to IgG1 in normal hamsters, I-hamsters, and L-I-hamsters were 1.44, 1.47, and 4.52 (Fig. 9, insets), respectively. Thus, L-I-hamsters showed a significant increase in the IgG2 level, indicating that there was development of an effective cellular immune response, which is an indirect measure of the Th1 type of response.

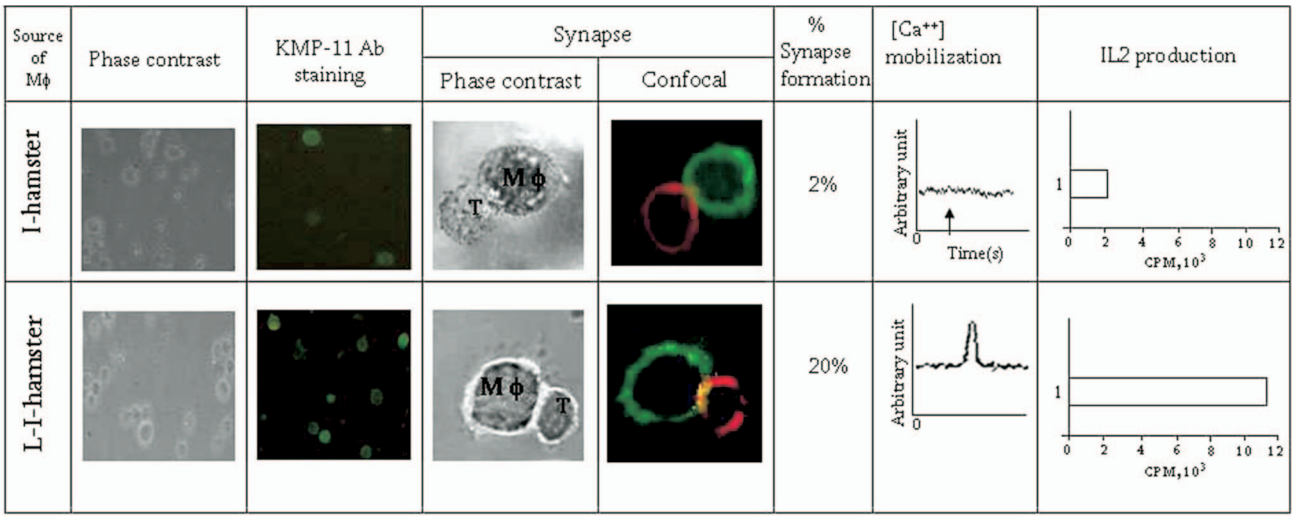

FIG. 6. Expression of the endogenous leishmanial antigen KMP-11 in MΦs derived from the splenocytes of I-hamsters and L-I-hamsters and their ability to form synapses with an anti-KMP-11 T-cell line (T^{KMP} cells). MΦs were stained with anti-KMP-11 MAb and were probed with FITC-labeled anti-mouse IgG. MΦs from normal hamsters did not show any staining with anti-KMP-11 Ab. To study synapse formation, MΦs were stained with CTXB-FITC, mixed with PKH26-labeled T^{KMP} cells, and kept at 37°C for 30 min. Conjugate formation was analyzed with a confocal microscope (Zeiss model LSM 510), and the results were expressed as percentages of synapse formation. Cells found in joint couplets by phase-contrast microscopy and exhibiting a zone of colocalization as determined by confocal microscopy were considered to have formed a synapse. The number of synapse-forming couplets per 100 APCs is expressed as the percentage of synapse formation. To study the extent of true synapse formation, fura-2-loaded T^{KMP} cells were mixed with MΦs, and fluorescence was monitored in real time to determine the intracellular Ca^{2+} mobilization. In a separate experiment using a similar setup, MΦs were mixed with T^{KMP} cells, and the resulting IL-2 production in the supernatant was monitored for the IL-2-dependent cell line HT-2. Growth of HT-2 cells was monitored by using [^{3}H]thymidine incorporation.

Cholesterol liposomes cured infected hamsters in the long run. The "gold standard" for clinical cure of kala azar is microscopic determination of the absence of the parasite in splenic aspirate (11, 63). We performed a microscopic evaluation to detect parasites in stamp smears. For this purpose 25 I-hamsters, 20 L-I-hamsters, and 20 L-I-sub-SAG-hamsters were used to study the survival kinetics. The I-hamsters had a maximum life span of 6 months; 80% of these hamsters sur-

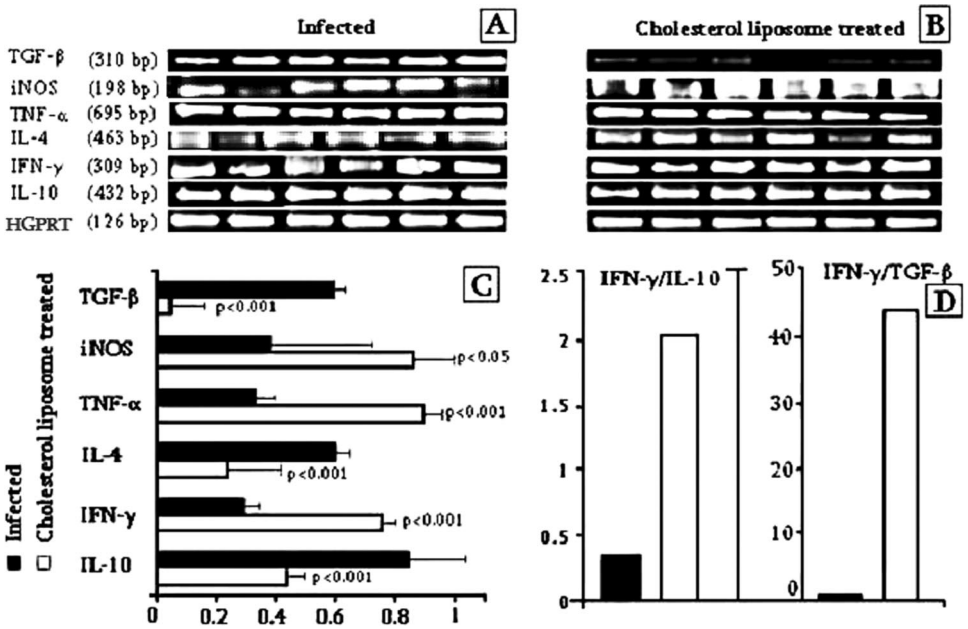

FIG. 7. Semiquantitative RT-PCR cytokine (TGF-β, TNF-α, IL-4, IFN-γ, and IL-10), iNOS, and HGPRT profiles for the splenocytes of I-hamsters and L-I-hamsters ($n = 6$). Equivalent amounts of RNA from splenic tissues of two groups of hamsters were used as the input for RT-PCR analysis, where the HGPRT gene was used as the housekeeping control gene. Expression of each cytokine transcript was expressed as a ratio of cytokine mRNA to HGPRT mRNA. The values obtained from densitometric analysis of each cytokine were expressed as means ± standard deviations instead of individual values. The ratios of IFN-γ to IL-10 and IFN-γ to TGF-β were analyzed for I-hamsters and L-I-hamsters. Two experiments were conducted separately, and the data show the results of a representative experiment.

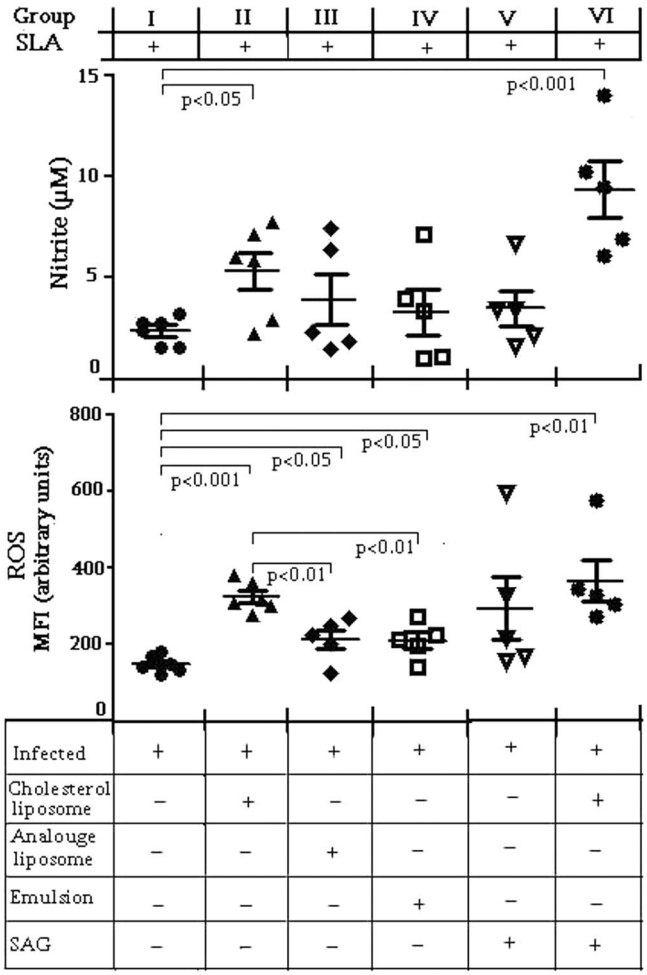

FIG. 8. Production of leishmanicidal effector molecules (NO and ROS) by splenocytes derived from different experimental groups of hamsters. The splenocytes were stimulated with SLA (5 μg/ml) and assayed for NO as described in Materials and Methods. ROS generation was measured by 2′,7′-dichlorodihydrofluorescein diacetate staining of splenocytes from different experimental groups. Three experiments were conducted separately, and the data show the results of a representative experiment. The groups indicated at the top are the groups described in the legend to Fig. 2. MFI, mean fluorescence intensity.

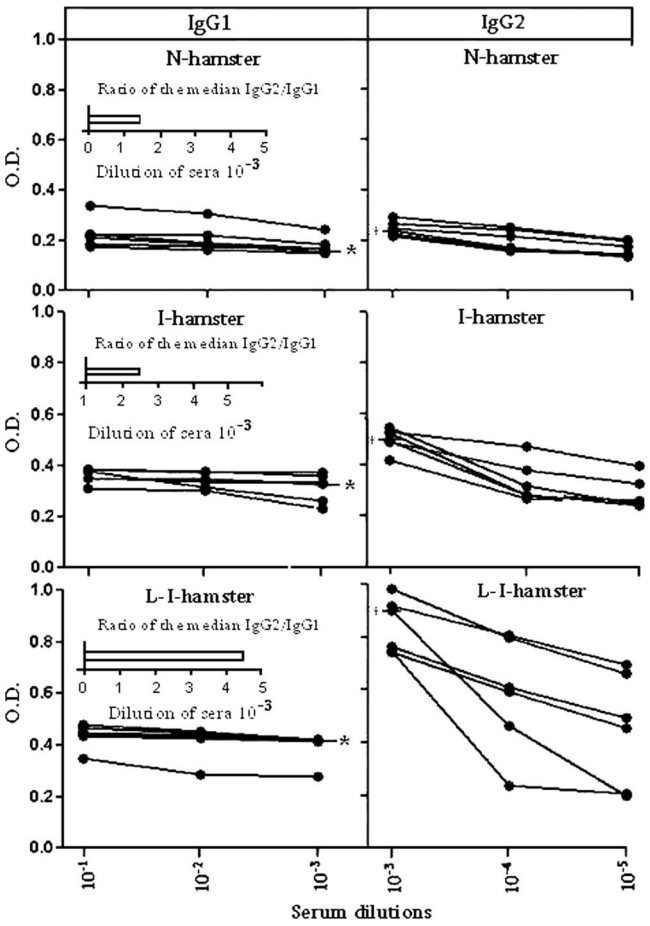

FIG. 9. Antileishmanial IgG1 and IgG2 Ab titers in different groups of hamsters (normal hamsters, I-hamsters, and L-I-hamsters). Sera of individual hamsters were assayed to determine the Ab titer by ELISA. The insets show the median IgG2/IgG1 ratios at a 10^{-3} dilution of sera between I-hamsters and L-I-hamsters. O.D., optical density.

vived up to 2 months, 60% survived up to 4 months, and 20% survived beyond 5 months and died by 6 months postinfection. On the other hand, 92% of L-I-hamsters and 100% L-I-sub-SAG-hamsters remained alive until the termination of experiment (Fig. 10A). After termination of the experiment (i.e., at 9 months postinfection), seven animals from each group were investigated at random for parasites in the spleen and liver. Remarkably, no amastigotes could be detected by microscopy in impressions of Giemsa-stained tissue stamp smears of transverse sections of the spleen and liver. Experiments performed at random with three hamsters showed that the organ weights returned to normal (Fig. 10B), while all three hamsters showed high titers of antileishmanial IgG2 and, to a lesser extent, of IgG1 (Fig. 10C and D), suggesting that the hamsters were indeed infected with *L. donovani* and the antileishmanial immune repertoire was intact.

DISCUSSION

Our study very clearly showed that a single injection of cholesterol liposomes into I-hamsters (infected with either promastigotes or amastigotes) caused a significant reduction in the parasite burden in the spleen and liver. The therapeutic effect was further enhanced when cholesterol liposomes was combined with sub-SAG, indicating that this combination may be considered for reducing the dose of chemotherapeutic agents in general. In this investigation cholesterol-rich unilamellar liposomes were used because of a number of compelling attributes: (i) this system is an ideal system for delivering cholesterol to the host cells because of the concentration (thermodynamic) gradient (51); (ii) the half-life of the cholesterol-rich unilamellar liposomes is longer than that of cholesterol-poor liposomes in the body fluid (32); (iii) small unilamellar liposomes that are a defined size (70 to 80 nm) are believed to be targeted to hepatic cells more efficiently than multilamellar vesicles (13) and theoretically allow passage through large fenestrations, such as those of sinusoidal capillaries (19); and (iv) while in circulation, liposomes readily absorb a vast collection

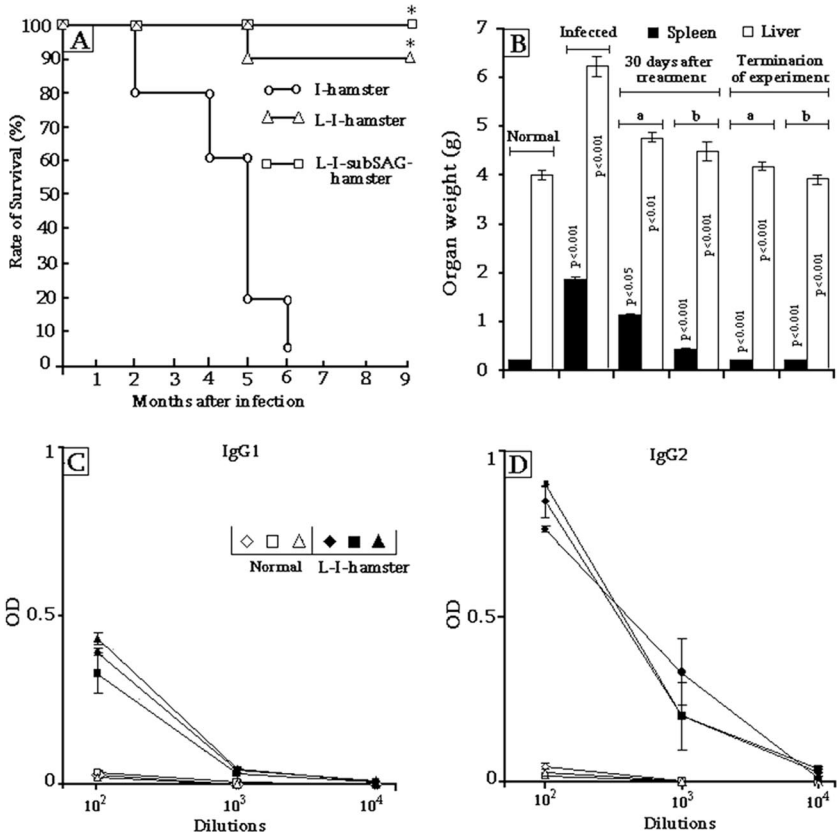

FIG. 10. Long-term survival of I-hamsters, L-I-hamsters, and L-I-sub-SAG-hamsters. (A) Percentages of survival. The asterisks indicate when hamsters were sacrificed. (B) Organ weight (spleen and liver) for I-hamsters, L-I-hamsters, and L-I-sub-SAG-hamsters (three hamsters were chosen at random from each group). Three-month-old hamsters were used as the normal group as there was not much variation in organ weight after this. The organ weights (spleen and liver) were recorded 30 days after the hamsters received either cholesterol liposomes or cholesterol liposomes and sub-SAG and were compared to the data for the corresponding infected groups. The organ weights (spleen and liver) were also recorded at the time that the experiment was terminated. Bars a and b indicate organ weights for L-I-hamsters and L-I-sub-SAG-hamsters, respectively. Since all the I-hamsters were dead by 6 months postinfection, there was no infected control for groups that survived until termination of the experiment. (C and D) The antileishmanial IgG1 (C) and IgG2 (D) levels were determined at the termination of the experiment and were compared to the data for age-matched controls. Representative data for three hamsters are shown. The statistical significance for comparisons of normal and infected groups and of infected and protected groups are indicated. The error bars indicate standard deviations. OD, optical density.

of plasma proteins, some of which may act as opsonins directing liposomes to cell surface receptors and promoting their uptake by MΦs in the liver and spleen (17), the site of parasite replication.

The therapeutic effect was cholesterol specific because the analogue with the 3-β-hydroxyl function, 4-cholesten-3-one, failed to induce any effect. We used this analogue because the alignment of cholesterol in the membrane is thought to be supported by a hydrogen bond between the cholesterol OH group and the amide bond of sphingolipid (64) and this interaction is presumably not present in the case of this analogue because of the lack of an OH group. The fact that the analogue liposomes failed to provide any protection, unlike cholesterol liposomes, may be due to the inability of the analogue to stack in the membrane. Interestingly, injection of a lipid emulsion made up of cholesterol and PC at the same proportion as that in cholesterol liposomes failed to provide any protection, suggesting that the emulsion is either cleared rapidly from the circulation or is unable to transfer cholesterol to the host cells. It has been reported that liposomes made up of PC and stearylamine have no significant therapeutic effect in the *L. donovani*-infected mouse model (5), lending credence to the notion that the cholesterol liposomes have therapeutic ability.

Having established that cholesterol liposomes possess therapeutic potential in experimental leishmaniasis, we tried to determine the host factors in the protection process. Our study revealed that protected animals show strong antileishmanial T-cell proliferation, suggesting that there was expansion of the antileishmanial T-cell repertoire that was absent in analogue liposome- or emulsion-treated groups. Curiously, I-hamsters receiving analogue liposomes and emulsion responded to ConA but not to leishmanial antigen, whereas I-hamsters receiving cholesterol liposomes responded to both of these factors. This showed that cholesterol liposomes but not analogue liposomes favor expansion of antigen-specific T cells in I-hamsters. It was interesting that the polyclonal response to ConA triggered essentially the same growth response (proliferation) that leishmanial antigen triggered. This may have been due to the use of a higher concentration of ConA in our study than in other studies (46, 49). In the present investigation we used MΦs as a prototype of APCs because no hamster-specific reagents are available to generate dendritic cells. Furthermore,

intravenously injected liposomes target their content only to the MΦs that are in contact with circulating blood (i.e., Kupffer cells in the liver and several subpopulations of splenic MΦs) (53); fortuitously, these are the target cells where parasites replicate. This also showed that the cholesterol content of splenic I-MΦs was significantly lower than that of splenic L-I-MΦ, which was evident from quantitative determination of membrane cholesterol.

The impact of the decrease in membrane cholesterol on the T-cell-stimulating ability of I-MΦs was also assessed. Previously, we have shown that *L. donovani*-infected human monocytes can act as anti-KMP-11 peptide-specific cytotoxic T-lymphocyte targets without exogenous KMP-11 (7). The present study revealed that KMP-11 was expressed in both I-MΦs and L-I-MΦs as an endogenous antigen and that the signal was weaker in the former MΦs. We also studied the ability of I-MΦs and L-I-MΦs to form synapses with T^{KMP} cells in the absence of exogenous KMP-11. Their activation was measured utilizing intracellular Ca^{2+} mobilization and IL-2 production as a marker of true synapse formation as these two events go hand in hand (38). There are reports that endogenously derived leishmanial antigens can activate $CD4^+$ T cells (30) and $CD8^+$ T cells (31). In one investigation the microtubule organizing center was used as a marker of T-cell activation (41). However, we believe that Ca^{2+} mobilization is more sensitive because it is an upstream event required for microtubule assembly (39). The percentages of synapse formation with I-MΦs and L-I-MΦs were 2% and 20%, respectively; in the latter case both Ca^{2+} mobilization and IL-2 production were noted, suggesting that the synapses were true synapses. There has been a report that the accessibility of some membrane proteins is affected depending on a change in the membrane fluidity (45). The observation described above indicates the importance of membrane cholesterol for developing antileishmanial immunity and subsequent protection in *L. donovani*-infected hamsters.

The mechanism by which L-I-MΦs show enhanced binding of anti-KMP-11 Ab is not known. However, it is possible that the accessibility of anti-KMP-11 Abs may be due to the rigidity of the membrane, as shown by other workers with model membranes (26). An alternative possibility is that because of its ability to fold and unfold KMP-11 may interact with the membrane lipid (18). There is spectroscopic evidence showing that variation in the cholesterol concentration in the membrane can perturb the protein secondary structure; this has been well studied in photosystem II of chloroplasm (8) and in the cholecystokinin receptor (24).

We have noticed downregulation of the IL-10 mRNA level in L-I-hamsters compared to I-hamsters. The level of IL-10, a key MΦ-deactivating Th1-suppressive cytokine, is reported to increase during an acute phase of visceral leishmaniasis; cure is associated with a decrease in the level (20). It has also been suggested that TNF-α is one of the important agents that stimulate MΦs to produce NO (35). We observed significant increases in the levels of IFN-γ, TNF-α, and iNOS transcripts coupled with generation of ROS and NO in the splenocytes of L-I-hamsters compared to I-hamsters. However, the picture was a little different when NO generation and ROS generation were compared for the L-I-hamster, analogue-treated, and emulsion-treated groups. It was observed that there was significantly greater ROS generation in L-I-hamsters than in the other two groups. On the other hand, there was not much difference in NO production among these groups. Thus, it is reasonable to speculate that in cholesterol liposome-mediated protection ROS may play a more important role than NO. IFN-γ and TNF-α are often reported to act in concert to activate iNOS for the production of NO (36). We found significant downregulation of TGF-β in L-I-hamsters compared to infected controls. TGF-β has also been recognized as an important immunoregulator in murine leishmaniasis; it increases the susceptibility to disease (66). TGF-β suppresses IFN-γ-induced MHC class II expression by inhibiting class II transactivator mRNA (34), while cholesterol treatment attenuates or suppresses TGF-β responsiveness in all cell types studied (12). It has been shown by Anderson et al. (3) that the therapeutic efficacy of TGF-β neutralization is potentiated by simultaneous inhibition of IL-10 (3), indicating the importance of both of the cytokines in disease progression. We like to emphasize the possible role of TGF-β in the outcome of *L. donovani* infection in hamsters because the IFN-γ/TGF-β ratio changed dramatically compared to the IFN-γ/IL-10 ratio upon cholesterol liposome treatment.

In mice, IL-4 and IFN-γ are two cytokines that direct Ig class switching of IgG1 and IgG2a, respectively (62). Although there is no distinct classification of Igs in hamster, it is believed that hamster IgG2 corresponds to mouse IgG2a/IgG2b and hamster IgG1 corresponds to murine IgG1 (16). L-I-hamsters exhibit an effective immune response by showing substantially higher anti-SLA-specific IgG2 titers, which is a measure of the cell-mediated immune response. There was a significant increase in the IgG2/IgG1 ratio in the protected hamsters compared to the infected group. Therefore, our study was restricted to only a single injection. We used sub-SAG with cholesterol liposomes, which slightly enhanced the parasite clearance compared to cholesterol liposome treatment alone but failed to provide sterile protection at an early time point (1 month after liposome treatment). Therefore, we studied the long-term survival of the hamsters. From the mortality data it was clear that a single cholesterol liposome treatment increased the life expectancy of 92% of the hamsters, whereas combined therapy ensured 100% survival until termination of the experiments after 9 months. At that time point we determined the spleen and liver weights and also the parasite burden. Surprisingly, the organ weights were close to normal, and no parasites could be detected either in L-I-hamsters or in L-I-sub-SAG-hamsters by the stamp smear method. The protected hamsters showed the presence of antileishmanial Ab, indicating that they were indeed exposed to parasites. There was variation in the number of parasites in the spleens and livers in infected hamsters, the cause of which is not clear. But it seems likely that the variation in parasite burden may have occurred because the animals were not members of a pure inbred population. Syrian hamsters are believed to have the limited driving force characteristic of epizootics. To avoid any controversy concerning polymorphism of MHC molecules, ambiguous terms like "diversity" and "variation" are used in the literature. There is no clear-cut convincing data on the extent of polymorphism at both the class I and class II loci. However, there is some agreement that MHC class I of Syrian hamsters is essentially monomorphic (65).

In conclusion, it appears that the use of cholesterol as an adjunct might help reduce the doses and thereby the toxicities of the known antileishmanial drugs. The central conclusion from this work is that infection led to an increase in membrane fluidity as a consequence of a decrease in the level of membrane cholesterol and this possibly compromised the APC function. The cholesterol liposome-driven protective immunity may be the consequence of the corrected membrane fluidity of APCs. The resulting expansion of the antileishmanial T-cell repertoire and generation of host-protective cytokines coupled with production of oxygen and nitrogen intermediates culminated in killing of intracellular parasites. This finding does not exclude the possibility that cholesterol is incorporated into other host cells, including dendritic cells and T cells, upon cholesterol liposome treatment. But it is evident that cholesterol liposome treatment allows recovery of the immune response, which eventually wipes out the infection. The mechanism by which intracellular parasites modulate membrane cholesterol is not known. Obviously, it is necessary to take a mechanistic look at the event that favored the expansion of antileishmanial T-cell clones upon cholesterol liposome treatment. This promises to be another area for study of the disease mechanism and treatment of resistant cases as it focuses on the host rather than the parasite.

ACKNOWLEDGMENTS

We are extremely grateful to Paul Kaye, A. Bryceson, and B. Achari for critically reviewing the manuscript.

This work was supported by CSIR grant NWP0005. S.B., S.S., M.G., and A.H. were recipients of CSIR fellowships. J.G., R.G., and R.D. were recipients of UGC fellowships.

REFERENCES

1. **Amer, A. O., and M. S. Swanson.** 2002. Phagosome of one's own: a microbial guide to life in the macrophage. Curr. Opin. Microbiol. **5:**56–61.
2. **Amundson, D. M., and M. Zhou.** 1999. Fluorometric method for the enzymatic determination of cholesterol. J. Biochem. Biophy. Methods **38:**43–52.
3. **Anderson, F. C., R. Lira, S. Kamhawi, Y. Belkaid, T. A. Wynn, and D. Sacks.** 2008. Il-10 and TGF-β control the establishment of persistent and transmissible infections produced by *Leishmania tropica* in C57BL/6 mice. J. Immunol. **180:**4090–4097.
4. **Anderson, H. A., E. M. Hiltbold, and P. A. Roche.** 2000. Concentration of MHC class II molecules in lipid rafts facilitates antigen presentation. Nat. Immunol. **1:**156–162.
5. **Banerjee, A., M. De, and N. Ali.** 2008. Complete cure of experimental visceral leishmanisis with amphotericin B in stearylamine-bearing cationic liposomes involves down-regulation of IL-10 and favourable T cell responses. J. Immunol. **181:**1386–1398.
6. **Basu, R., S. Bhaumik, J. M. Basu, K. Naskar, T. De, and S. Roy.** 2005. Kinetoplastid membrane protein-11 DNA vaccination induces complete protection against both pentavalent antimonial-sensitive and -resistant strains of *Leishmania donovani* that correlates with inducible nitric oxide synthase activity and IL-4 generation: evidence for mixed Th1- and Th2-like responses in visceral leishmaniasis. J. Immunol. **174:**7160–7171.
7. **Basu, R., S. Roy, and P. Walden.** 2007. HLA class I-restricted T cell epitopes of the kinetoplastid membrane protein-11 presented by *Leishmania donovani*-infected human macrophages. J. Infect. Dis. **195:**1373–1380.
8. **Bograh, A., R. Carpentier, and H. A. Tajmir-Riahi.** 1999. The effect of cholesterol on the solution structure of proteins of photosystem II. Protein secondary structure and photosynthetic oxygen evolution. J. Colloid Interface Sci. **210:**118–122.
9. **Burger, K., G. Gimpl, and F. Farenholz.** 2000. Regulation of receptor function by cholesterol. Cell. Mol. Life Sci. **57:**1577–1592.
10. **Chakraborty, D., S. Banerjee, A. Sen, K. K. Banerjee, P. Das, and S. Roy.** 2005. *Leishmania donovani* affects antigen presentation of macrophage by disrupting lipid rafts. J. Immunol. **175:**3214–3224.
11. **Chappuis, F., S. Sundar, A. Hailu, H. Galib, S. Rijal, R. W. Peeling, J. Alvar, and M. Boelaert.** 2007. Visceral leishmaniasis: what are needed for diagnosis, treatment and control? Nat. Rev. Microbiol. **5:**S7–S16.
12. **Chen, C. L., I. H. Liu, S. J. Fliesler, X. Han, S. S. Huang, and J. S. Huang.** 2007. Cholesterol suppresses cellular TGF-β responsiveness: implications in atherogenesis. J. Cell Sci. **120:**3509–3521.
13. **Chow, D. D., H. E. Essien, M. M. Padki, and K. J. Hwang.** 1989. Targeting small unilamellar liposomes to hepatic parenchymal cells by dose effect. J. Pharmacol. Exp. Ther. **248:**506–513.
14. **Croft, S. L., S. Sundar, and A. H. Fairlamb.** 2006. Drug resistance in leishmaniasis. Clin. Microbiol. Rev. **19:**111–126.
15. **Dabrowski, M. P., W. E. Peel, and A. E. R. Thomson.** 1980. Plasma membrane cholesterol regulates human lymphocyte cytotoxic function. Eur. J. Immunol. **10:**821–827.
16. **Elias, E. R., M. B. Irons, A. D. Hurley, G. S. Tint, and G. Salen.** 1997. Clinical effects of cholesterol supplementation in six patients with the Smith-Lemli-Opitz syndrome (SLOS). Am. J. Med. Genet. **68:**305–310.
17. **Fielding, R. M., L. Moon-McDermott, R. O Lewis, and M. J. Horner.** 1999. Pharmacokinetics and urinary excretion of amikacin in low-clearance unilamellar liposomes after a single or repeated intravenous administration in the rhesus monkey. Antimicrob. Agents Chemother. **43:**503–509.
18. **Fuertes, M. A., C. Berherich, R. M. Lozano, G. Gimenez-Gallego, and C. Alonso.** 1999. Folding stability of the kinetoplastid membrane protein-11 (KMP-11) from *Leishmania infantum*. Eur. J. Biochem. **260:**559–567.
19. **Gabizon, A., and D. Papahadjopoulos.** 1988. Liposome formulations with prolonged circulation time in blood and enhanced uptake by tumors. Proc. Natl. Acad. Sci. USA **85:**6949–6953.
20. **Ghalib, H. W., M. R. Piuvezam, Y. A. Skeiky, M. Siddig, F. A. Hashim, A. M. el-Hassan, D. M. Russo, and S. G. Reed.** 1993. Interleukin 10 production correlates with pathology in human *Leishmania donovani* infections. J. Clin. Investig. **92:**324–329.
21. **Ghosh, M., C. Pal, M. Ray, S. Maitra, L. Mandal, and S. Bandyopadhyay.** 2003. Dendritic cell-based immunotherapy combined with antimony-based chemotherapy cures established murine visceral leishmaniasis. J. Immunol. **170:**5625–5629.
22. **Green, L. C., D. A. Wanger, J. Glogowski, P. L. Skipper, J. S. Wishnok, and S. R. Tannenhaum.** 1982. Analysis of nitrate, nitrite, and [^{15}N] nitrate in biological fluids. Anal. Biochem. **126:**131–138.
23. **Griffith, J. M., and G. Posthuma.** 2002. A reliable and convenient method to store ultrathin thawed cryosections prior to immunolabeling. J. Histochem. Cytochem. **50:**57–62.
24. **Harikumar, K. G., V. Puri, R. Singh, K. Hanada, R. E. Pagano, and L. J. Miller.** 2005. Differential effects of modification of membrane cholesterol and sphingolipids on the conformation, function and trafficking of the G protein-coupled cholecystokinin receptor. J. Biol. Chem. **280:**2176–2185.
25. **Hughes, D. A., P. J. Townsend, and P. L. Haslam.** 1992. Enhancement of antigen presenting function of monocytes by cholesterol: possible relevance to inflammatory mechanisms in extrinsic allergic alveolitis and atherosclerosis. Clin. Exp. Immunol. **87:**279–286.
26. **Humphries, G. M. K., and H. M. McConnell.** 1977. Membrane-controlled depletion of complement activity by spin-label-specific IgM. Proc. Natl. Acad. Sci. USA **74:**3537–3541.
27. **Kalipatnapu, S., and A. Chattopadhyay.** 2007. Membrane organization of the serotonin 1A receptor monitored by a detergent-free approach. J. Cell. Mol. Neurobiol. **27:**463–474.
28. **Kaye, P. M., M. Svensson, M. Ato, A. Maroof, R. Polley, S. Stager, S. Zubairi, and C. R. Engwerda.** 2004. The immunopathology of experimental visceral leishmaniasis. Immunol. Rev. **201:**239–253.
29. **Keithly, J. S.** 1976. Infectivity of *Leishmania donovani* amastigotes and promastigotes for golden hamsters. J. Protozool. **23:**244–245.
30. **Kima, P. E., L. Soong, C. Chicharro, N. H. Ruddle, and D. P. McMahon-Pratt.** 1996. Leishmania-infected macrophages sequester endogenously synthesized parasite antigens from presentation to CD4$^+$ T cells. Eur. J. Immunol. **26:**3163–3169.
31. **Kima, P. E., N. H. Ruddle, and D. McMohan-Pratt.** 1997. Presentation via class I pathway by Leishmania amazonensis infected macrophages of an endogenous leishmanial antigen to CD8$^+$ T-cells. J. Immunol. **159:**1828–1834.
32. **Kirby, C., J. Clarke, and G. Gregoriadis.** 1980. Effect of the cholesterol content of small unilamellar liposomes on their stability in vivo and in vitro. Biochem. J. **186:**591–598.
33. **Lal, C. S., A. Kumar, S. Kumar, K. Panday, N. Kumar, S. Bimal, P. K. Sinha, and P. Das.** 2007. Hypocholesterolemia and increased triglyceride in paediatric visceral leishmaniasis. Clin. Chim. Acta **382:**151–153.
34. **Lee, Y. J., Y. Han, H T. Lu, V. Nguyen, H. Qin, P. H. Howe, B. A. Hocevar, J. M. Boss, R. M. Ransohoff, and E. N. Benveniste.** 1997. TGF-beta suppresses IFN-gamma induction of class II MHC gene expression by inhibiting class II transactivator messenger RNA expression. J. Immunol. **158:**2065–2075.
35. **Liew, F. Y., Y. Li, and S. Millott.** 1990. Tumour necrosis factor-α synergizes with IFN-γ in mediating killing of *Leishmania major* through the induction of nitric oxide. J. Immunol. **145:**4306–4310.
36. **Liew, F. Y., Y. Li., and S. Millott.** 1990. Tumour necrosis factor (TNF-α) in leishmaniasis. II. TNF-α-induced macrophage leishmanicidal activity is mediated by nitric oxide from L-arginine. Immunology **71:**556–559.
37. **Lowry, O. H., N. J. Rosebrough, A. L Farr, and R. J. Randall.** 1951. Protein measurement with the Folin phenol reagent. J. Biol. Chem. **193:**265–275.
38. **Makino, M., Y. Sei, P. K. Arora, H. C. Morse III, and J. W. Hartley.** 1992.

Impaired Ca^{2+} mobilization in $CD4^+$ and $CD8^+$ T-cells in a retrovirus-induced immunodeficiency syndrome, murine AIDS. J. Immunol. **149:**1707–1713.
39. **Marcum, J. M., J. R. Dedman, B. R. Brinkley, and A. R. Means.** 1978. Control of microtubule assembly-disassembly by calcium-dependent regulator protein. Proc. Natl. Acad. Sci. USA **75:**3771–3775.
40. **Medda, S., N. Das, B. K. Bachhawat, S. B. Mahato, and M. K. Basu.** 1990. Targeting of plant glycoside-bearing liposomes to specific cellular and subcellular sites. Biotechnol. Appl. Biochem. **12:**537–543.
41. **Meier, C. L., M. Svensson, and P. M. Kaye.** 2003. *Leishmania*-induced inhibition of macrophage antigen presentation analyzed at the single-cell level. J. Immunol. **171:**6706–6713.
42. **Melby, P. C., V. V. Tryon, B. Chandrasekar, and G. L. Freeman.** 1998. Cloning of Syrian hamster (*Mesocricetus auratus*) cytokine cDNAs and analysis of cytokine mRNA expression in experimental visceral leishmaniasis. Infect. Immun. **66:**2135–2142.
43. **Mukherjee, S. B., M. Das, G. Sudhandiran, and C. Shaha.** 2002. Increase in cytosolic Ca^{2+} levels through the activation of non-selective cation channels induced by oxidative stress causes mitochondrial depolarization leading to apoptosis-like death in *Leishmania donovani* promastigotes. J. Biol. Chem. **277:**24717–24727.
44. **Mukhopadhyay, S., P. Sen, S. Bhattacharyya, S. Majumdar, and S. Roy.** 1999. Immunoprophylaxis and immunotherapy against experimental visceral leishmaniasis. Vaccine **17:**291–300.
45. **Muller, C. P., D. A. Stephany, M. Shinitzky, and J. R. Wunderlich.** 1983. Changes in cell surface expression of MHC and Thy 1.2 determinants following treatment with lipid modulating agents. J. Immunol. **131:**1356–1362.
46. **Nelles, M. J., W. R. Duncan, and J. W. Streilein.** 1981. Immune response to acute virus infection in the syrian hamster. II. Studies on the identity of virus induced cytotoxic effector cells. J. Immunol. **126:**214–218.
47. **Neogy, A. B., A. Nandy, B. G. Dastidar, and A. B. Chowdhury.** 1988. Modulation of the cell-mediated immune response in kala-azar and post-kala-azar dermal leishmaniasis in relation to chemotherapy. Ann. Trop. Med. Parasitol. **82:**27–34.
48. **Perez-Guzman, C., M. H. Vargas, F. Quinonez, N. Bazavilvazo, and A. Aguilar.** 2005. A cholesterol-rich diet accelerates bacteriological sterilization in pulmonary tuberculosis. Chest **127:**643–651.
49. **Peters, B. A., M. Sothmann, and W. B. Wehrenberg.** 1989. Blood leukocyte and spleen lymphocyte immune response in chronically physically active and sedentary hamsters. Life Sci. **45:**2239–2245.
50. **Pucadyil, T. J., and A. Chattopadhyay.** 2007. Cholesterol: a potent therapeutic target in Leishmania infection? Trends Parasitol. **23:**49–53.
51. **Radhakrishnan, A., and H. M. McConnell.** 2000. Chemical activity of cholesterol in membranes. Biochemistry **39:**8119–8124.
52. **Razzaq, T. M., P. Ozebge, E. C. Jury, P. Sembi, N. M. Blackwell, and P. S. Kabouridis.** 2004. Regulation of T-cell receptor signaling by membrane microdomain. Immunology **113:**413–426.
53. **Rooijen, N. V., and A. Sanders.** 1998. The macrophage as target or obstacle in liposome based target strategies. Int. J. Pharm. **162:**45–50.
54. **Roy, S., G. Terres, and S. Leskowitz.** 1987. The azobenzenearsonate conjugate of poly-glutamic-lysine-tyrosine will induce tyrosine-azobenzenearsonate-specific T-cell responses and clones in nonresponder mice. Cell. Immunol. **105:**118–126.
55. **Roychoudhury, K., B. Dasgupta, P. Sen, T. Laskay, W. Solbach, T. De, and S. Roy.** 2006. Evidence of direct interactions between the CC-chemokines CCL3, CCL4 and CCL5 and Leishmania promastigotes. Mol. Biochem. Parasitol. **150:**374–377.
56. **Saha, B., D. Bandyopadhyay, and S. Roy.** 1995. Immunobiological studies on experimental visceral leishmaniasis. IV. Kinetics of evolution of disease promoting versus host protective cells of monocytes, macrophage lineage and their characterization. Scan. J. Immunol. **42:**540–546.
57. **Saha, B., H. N. Roy, A. Pakrashi, R. N. Chakrabarti, and S. Roy.** 1991. Immunobiological studies on experimental visceral leishmaniasis. I. Changes in lymphoid organs and their possible role in pathogenesis. Eur. J. Immunol. **21:**577–581.
58. **Silvestre, R., A. Cordeiro-Da-Silva, N. Santarem, B. Vergnes, D. Sereno, and A. Ouaissi.** 2007. SIR2-deficient *Leishmania infantum* induces a defined IFN-γ/IL-10 pattern that correlates with protection. J. Immunol. **179:**3161–3170.
59. **Simons, K., and E. Ikonen.** 2000. How cells handle cholesterol. Science **290:**1721–1726.
60. **Slotte, J. P., and B. Lundberg.** 1983. Effects of cholesterol surface transfer on cholesterol and phosphatidyl choline synthesis in cultured rat arterial smooth muscle cells. Med. Biol. **61:**223–227.
61. **Stauber, L. A.** 1958. Host resistance to the Khartoun strain of *Leishmania donovani*. Rice Inst. Pam. **45:**80–96.
62. **Stevens, T. L., A. Bossie, V. M. Sanders, R. Fernandez-Botran, R. L. Coffman, T. R. Mosmann, and E. S. Vitetta.** 1988. Regulation of antibody isotype secretion by subsets of antigen specific T-helper cells. Nature **334:**255–258.
63. **Sundar, S., T. K. Jha, C. P. Thakur, P. K. Sinha, and S. K. Bhattacharya.** 2007. Injectable paramomycin for visceral leishmaniasis in India. N. Engl. J. Med. **356:**2571–2581.
64. **van der Goot, F. G., and T. Harder.** 2001. Raft membrane domains: from a liquid ordered membrane phase to a site of pathogen attack. Semin. Immunol. **13:**89–97.
65. **Watkins, D. I., Z. W. Chen, A. L. Hughes, A. Lagos, A. M Lewis, Jr., J. A. Shadduck, and N. L. Letvin.** 1990. Syrian hamsters express diverse MHC class I gene products. J. Immunol. **145:**3483–3490.
66. **Wilson, M. E., B. M. Young, B. L. Davidson, K. A. Mante, and S. E. McGowan.** 1998. The importance of TGF-β in murine visceral leishmaniasis. J. Immunol. **161:**6148–6155.
67. **World Health Organization.** 2006. Control of leishmaniasis. Report by the Secretariat. World Health Organization, Geneva, Switzerland.
68. **Wunder, C., Y. Churin, F. Winau, D. Warnecke, M. Vieth, B. Lindner, U. Zahringer, H.-J. Mollenkopf, E. Heinz, and T. F. Meyer.** 2006. Cholesterol glucosylation promotes immune evasion by *Helicobacter pylori*. Nat. Med. **12:**1030–1038.
69. **Zerpa, O., M. Ulrich, M. Polegre, A. Avila, O. N. Matos, I. Mendoza, F. Pratlong, C. Ravel, and J. Convit.** 2007. Diffuse cutaneous leishmaniasis responds to miltefosine but then relapses. Br. J. Dermatol. **156:**1328–1335.

Editor: W. A. Petri, Jr.